Front. Earth Sci. 2024, 18(3): 554–564
https://doi.org/10.1007/s11707-022-1080-4

RESEARCH ARTICLE

Spatial statistical analysis of earthquakes in the Fethiye - Burdur fault zone

Kerem HEPDENIZ (✉)

Department of Architecture and Urban Planning, Bucak EG Technical Sciences and Vocational School of Higher Education, Mehmet Akif Ersoy University, Burdur 15030, Turkey

Abstract Turkey is located in the Alpine-Himalayan seismic zone. The Anatolian plate has witnessed very severe and destructive earthquakes both in the past and today. In this study, statistical analyses of earthquakes that occurred between 1914 and 2019 along the Fethiye-Burdur fault zone, which is an active line, were conducted using geographic information systems. Analyses of standard distance, standard deviational eclipse, mean center, and median center were conducted to determine the geographic distributions of epicenters with a magnitude value of 3.5 and above. Quadrat and Average Nearest Neighbor analyses were used to reveal the spatial pattern. Anselin Local Moran I and Getis Ord Gi* method were used to determining where the earthquake epicenters are clustered locally. Kernel Density analyses were conducted to measure earthquake epicenters' density. Quadrat analysis, Average Nearest Neighbor, Global Moran's *I*, and Getis - Ord General G indices demonstrated that earthquakes are clustered in certain regions and are related to each other positionally. Anselin Moran's I regional analyses revealed that high values were clustered in the West of Burdur city center and the district of Yeşilova, and similar results were obtained in the Getis Ord Gi* method.

Keywords earthquake, Geographic Information Systems, spatial analysis, Fethiye-Burdur fault zone, Turkey

1 Introduction

Most of its land is in Asia, Turkey has a surface area of 780000 km^2. Due to its geological, meteorological and topographic structure, it is frequently exposed to natural disasters. Among these natural disasters, earthquakes rank first in terms of loss of life and property. When we look at the major earthquakes that have occurred since 1900, it ranks fourth in the world with 77 earthquakes (Afad, 2018).

The N-S extensional West Anatolian and Aegean plate is moving toward the south-west at a speed of about 15 − 30 mm/year along with the Fethiye-Burdur fault zone (FBFZ), where the study area is also included (McClusky et al., 2000; Yılmaz, 2000; Koukouvelas and Aydın, 2002). FBFZ covers an area of approximately 300 km, north-east-south-west, trending between the Gulf of Fethiye and Lake Burdur in Turkey's south-western region (Fig. 1). FBFZ, one of the important areas of active deformation in Turkey, and regional neotectonic features of South-western Anatolia have been investigated by many researchers (McKenzie, 1978; Koçyigit, 1983; Karaman, 1986, 1990; Taymaz and Price, 1992; Barka et al., 1997; Yagmurlu, 2000; Senturk, 2003; Beyhan and Keskinsezer, 2016). FBFZ, the subject of this study, forms the west wing of the Isparta angle. The Isparta Angle is a regional geological structure formed due to the autochthonous Taurus carbonate axis bending in the north of the Gulf of Antalya and around Isparta in an inverted "V" shape. This structure has a length of 180 km in the N-S direction and a width of approximately 100 km in the E-W direction. The fault systems between Fethiye and Lake Burdur were classified into three main groups NE-SW, NW-SE, and N-S. FBFZ is characterized by various segments and ages affecting the Mesozoic sequence and ophiolites of the Lycian nappes and Plio-Quaternary sediments in the Burdur Basin (Bering, 1971; Price and Scott, 1994). They found the existence of four main segments in this zone, delimited by NW-trending faults. These segments, from south-west to north-east, are 1) the Fethiye segment, 2) the Gölhisar segment, 3) the Tefenni segment, and 4) the Burdur segment. Burdur and Tefenni segments, 60–70 km long, are the most active structures farther compartmentalized into segments (Bering, 1971; Price and Scott, 1994; Bozcu et al., 2007; Beyhan and

Received August 26, 2023; accepted February 15, 2024

E-mail: khepdeniz@gmail.com

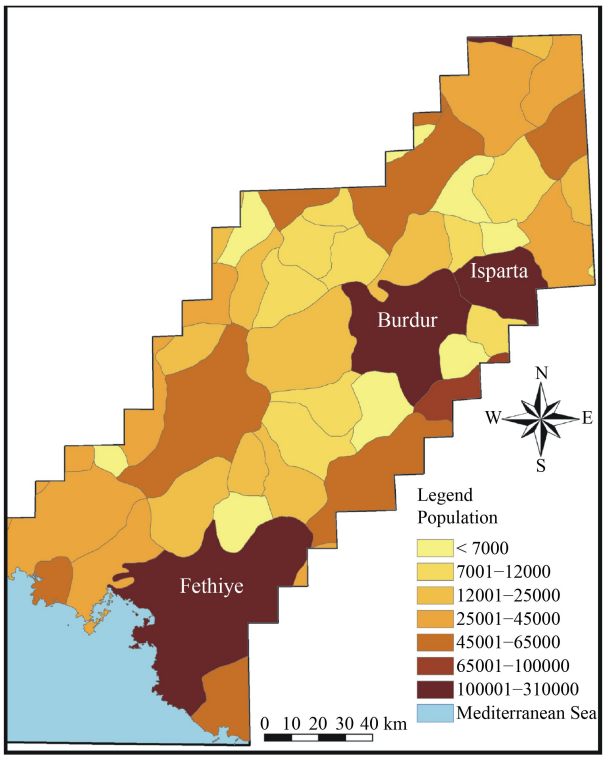

Fig. 1 Study area and population distribution.

Keskinsezer, 2016). Two large earthquakes of 7.1 and 6.2 magnitudes occurred in these segments in 1914 and 1971, while a 7.1 magnitude earthquake occurred in the southwest of Fethiye Bay in 1957 (Tan et al., 2008; Ozata, 2009; Tiryakioglu et al., 2013). In the earthquake of 1914, 2344 people died, and 681 were injured in the provinces of Burdur and Isparta. While the number of demolished houses in Burdur Province was close to 2000 (Ozata, 2009), 4175 out of 5100 houses became uninhabitable in Isparta (Sezer, 2014). The number of buildings damaged in the second large earthquake of 1971 in Burdur Province was 3227 (Ozyıldıran, 2015), while 57 casualties were declared (UCLEA, 2012). In the Fethiye earthquake in 1957, the death toll was 67, and the number of damaged buildings was reported to be 3100 (Atabey, 2000; Arslan, 2017).

Studies show that large earthquakes cluster temporally and spatially in certain periods (Bufe and Perkins, 2005; Ammon et al., 2010) and that many have been reported to be associated with fault zones (Kagan and Jackson, 1991; Stein et al., 1997; Tagıl and Alevkayalı, 2013). Due to their point distribution, the epicenters of earthquakes in a selected geographic region can be analyzed using geostatistical methods. As a result of these analyses, it can be revealed whether the epicenter points show a random, clustering, or scattering distribution.

The study aims to make GIS-based spatial analyses of earthquakes between 1914 and 2019 along the Fethiye-Burdur fault zone and to produce density maps. For this purpose, data from 1234 earthquakes with a magnitude of more than 3.5 that occurred around the Feyhiye-Burdur fault zone between 1914 and 2019 were obtained from the Boğaziçi Kandilli Observatory and Earthquake Research Institute, and spatial analysis was carried out with the specified methods. From the results, maps were produced and visualized, and risk areas were tried to be determined. In establishing the boundaries of the study area, the limit determined by Hall et al. (2014) was taken into account.

2 Spatial data

Seismic data on the region within the study area were obtained from the earthquake query system of Boğaziçi University Kandilli Observatory. The query process consists of 1234 earthquakes with a magnitude value between 3.5 and 7.1 between 1914 and 2019. Latitude and longitude coordinate data were converted to point data to analyze the data in Excel format within the scope of GIS. Point data outside the boundaries of the Fethiye-Burdur fault zone were found and eliminated while the ArcGIS 10 program was added to the database. This way, the occurrence date, time, coordinate values, depth, and magnitude values of earthquakes belonging to each earthquake point were transferred into the database. The spatial distributions of earthquakes that occurred within the study area between 1914 and 2019 can be seen in Fig. 2. In addition, spatial earthquake analyses were separated into groups of 3.5–4, 4–5, 5–6, and 6–7.1 according to their magnitudes.

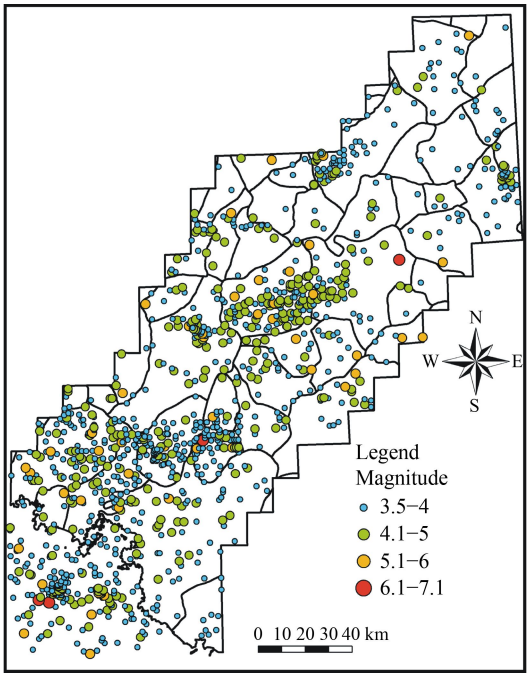

Fig. 2 Spatial distribution of earthquakes.

3 Materials and methods

To better understand our dynamic world, we need some simple models. To this end, we create models of the real world. In this way, we can better focus on the problems at hand. Statistics are needed to find the relationships between geographical and attribute data and summarize and add meaning to them. In this study, point pattern analysis, one of the geostatistical techniques, was used. Using the point pattern analysis, it is possible to determine where the points are concentrated in a way that the earthquake epicenters are defined or weighted based on a specific feature. These methods, which are used to evaluate the distribution, can also be used for purposes such as determining earthquake recurrence years; however, they cannot be used for earthquake risk analysis or prediction (Kasap and Gurlen, 2003). In this study, standard distance, standard deviational ellipse, mean center, and median center analyses were conducted to determine earthquakes' geographic distribution.

The spatial pattern of the measured density is revealed (Lee and Wong, 2001). In this study, the Quadrat analysis revealed the change in the distribution of earthquake epicenters.

Unlike Quadrat analysis, Average Nearest Neighbor (ANN) analysis compares mean distances observed in a known model with the nearest neighbor points. Accordingly, if the mean distance of earthquake epicenters is bigger than the random pattern, it is evaluated as scattered, whereas it is evaluated as clustering if it is smaller than the random pattern.

Quadrat and ANN analyses determine spatial models of point distributions and assume all points separately. Unlike these two methods, Moran's I analysis uses a measure known as the spatial correlation coefficient to measure and test the quality values of clustered or scattered earthquake points. Therefore, Moran's I method is more powerful and useful than Quadrat and ANN analyses (Lee and Wong, 2001). If the value of the Moran I index is lower than expected, it means that the epicenters have a scattered pattern, and if higher, they have a clustered pattern. Statistical significance for Moran's I was determined by calculating the Z score (Tagıl and Alevkayalı, 2013).

Getis-Ord General G (GOGG), a statistical method, was modeled by Getis and Ord as a statistical tool for analyzing spatial patterns (Getis and Ord, 1992). This study was used to determine the degree of clustering in earthquake epicenters.

Apart from global statistics, Anselin Local Moran's I, which is formed by similar and dissimilar variables, and Getis Ord Gi, which indicates where the hot spots and cold values are clustered positionally, were used to determine locally at which points earthquake epicenters were clustered. In contrast, Kernel Density analyses were used to measure earthquake epicenters' density.

3.1 Spatial statistical analyses

Spatial autocorrelation determines whether a feature obtained at a certain point is independent of the features obtained at neighboring positions. Spatial autocorrelation takes positive or negative values. While positive values demonstrate that features in neighboring positions affect each other linearly (clustering), negative values show that features in neighboring positions affect each other inversely (scattering) (Erdogan, 2010).

The mean center is the average of the x and y coordinates of the data in the study area. It is useful for tracking changes in data in the study area or comparing the distributions of different attribute types (Akyurek and Arslan, 2018). Earthquake epicenters form the center of gravity of the spatial distribution.

$$(X_{\mathrm{wmc}}, Y_{\mathrm{wmc}}) = \left(\frac{\sum_{i=1}^{n} w_i X_i}{\sum_{i=1}^{n} w_i}, \frac{\sum_{i=1}^{n} w_i Y_i}{\sum_{i=1}^{n} w_i} \right), \quad (1)$$

where, X_i and Y_i represent the position value of data paint, w_i represents the weight of the value at that position.

The median center defines the center point in the shortest distance with all data points in the data set (Mitchell, 2005). It provides important information about the direction of the distribution of the epicenter (Tagıl and Alevkayalı, 2013).

Standard distance measures the density or degree of scattering data points around the geometric mean center by circling the earthquake epicenters:

$$\mathrm{SD_w} = \sqrt{\frac{\sum_{i=1}^{n} f_i (x_i - xmc)^2 + \sum_{i=1}^{n} f_i (y_i - ymc)^2}{\sum_{i=1}^{n} f_i}}, \quad (2)$$

where, x_{mc} and y_{mc} represent the weighted mean center coordinates, f_i (x_i and y_i) represents the weight for the points (Lee and Wong, 2001).

The standard deviational ellipse is an effective tool to obtain the direction of earthquake epicenters. The distance in the standard deviational ellipse is calculated as the maximum and minimum axis. The deviation value of earthquake epicenters along the main axis indicates the maximum propagation direction; therefore, it also indicates whether earthquake points have a specific orientation (Mitchell, 2005).

In Quadrat analysis, the study area is divided into a regular square grid system, and the number of earthquake epicenters falling into these grids can form a frequency distribution. The change in the distribution of epicenters is compared with a random model formed theoretically. As a result, whether it is clustered or scattered can be found. The fact that all or most of the points fall within one or more grids indicates excessive clustering, while all grids containing a relatively similar number of points indicate a scattered pattern. The following formula calculates the mean-variance ratio (VMR):

$$\mathrm{VMR} = \frac{s^2}{x}, \tag{3}$$

where, s is the variance of the number of points per quadrat, and x is the mean of the number of points per quadrat.

If VMR is > 1, the model is clustered; if VMR equals 1, the model is random; if VMR is < 1, it means that the model is regular. Quadrat resolution may affect results. The suitable quadrate size for the study area was calculated using the following formula:

$$\mathrm{QS} = \frac{2 \times a}{n}, \tag{4}$$

where, a represents the study area, whereas n represents the number of earthquake epicenters (Lee and Wong, 2001).

ANN method predicts and averages the distance between the nearest neighbor and the position of each data in the data set. If the calculated mean distance is less than the mean of a hypothetical random distribution, the distribution of analyzed features is considered clustered, or if greater, the features are considered scattered.

To test whether any distribution is clustering, scattering, or random:

$$R = \frac{r_o}{r_e}, \tag{5}$$

the above formula has been used. r_o represents the mean of the observed distance between each earthquake epicenter and its nearest neighbor:

$$r_o = \frac{\sum_{i=1}^{n} r_i}{n}. \tag{6}$$

r_e is the expected mean distance for the randomly distributed earthquake epicenters and calculated by the following formula:

$$r_e = \frac{1}{\sqrt[2]{n/A}}. \tag{7}$$

In these formulas, r_i provides the closest distance between earthquake points, whereas n provides the number of earthquake epicenters, and A is the size of the study area.

ANN calculates the nearest neighbor index value based on the mean distance to the nearest neighbor of each data (only x and y coordinates) and their corresponding z values. If this value is less than 1, the pattern in the study area indicates clustering. If the index is greater than 1, the pattern tends to be scattered. The Z score or the standard deviation measure indicates statistical significance. If the Z score in the analysis is not between − 1.96 and 1.96, the pattern shows scattering ($p < 0.05$). If the Z score is between − 1.96 and 1.96, the pattern shows a random distribution (Getis and Ord, 1992; Lee and Wong, 2001; Mitchell, 2005; Erdogan, 2010; Akyurek and Arslan, 2018).

The General Moran's Index (GMI) statistic is a degree of spatial autocorrelation based on the positions of values and event-related values. GMI statistic shows the degree of spatial autocorrelation or the degree of scattering for a particular point pattern (Al-Ahmadi et al., 2014; Affan et al., 2016; Akyurek and Arslan, 2018).

$$I = \frac{n}{S_o} \frac{\sum_{i=1}^{n} \sum_{j=1}^{n} w_{i,j} Z_i Z_j}{\sum_{i=1}^{n} z_i^2}, \tag{8}$$

where, z_i is the deviation of the first earthquake epicenter from its mean value. $w_{i,j}$ represents the spatial weight between i and j values, n represents the total number of features, and S_o represents the sum of all weight values.

Getis and Ord modeled the GOGG statistic, and GOGG aims to determine the cluster size to find out whether there are hot spots (high-value clusters) or cold spots (low-value clusters) (Getis and Ord, 1992; Ord and Getis, 1995; Mitchell, 2005; Erdogan, 2010; Al-Ahmadi et al., 2014; Affan et al., 2016; Akyurek and Arslan, 2018). When the Z value is positive, the observed GOGG value is greater than the expected GOGG value; therefore, it can be said that high values for the relevant feature form clusters. When the Z score value is negative, the observed GOGG value is lower than the expected value (Al-Ahmadi et al., 2014; Affan et al., 2016).

$$\mathrm{G} = \frac{\sum_{i=1}^{n} \sum_{j=1}^{n} w_{i,j} X_i X_j}{\sum_{i=1}^{n} \sum_{j=1}^{n} x_i x_j}, \forall_{j \neq I.} \tag{9}$$

Information on x_ith, x_jth data, and jth data represent the weight coefficient between w_i, j_i, and j values, whereas n represents the total data.

Kernel density is a popular method used in statistical and geostatistical analysis and research. It is also frequently used in earthquake studies (Woo, 1996; Danese et al., 2008; Ayday et al., 2015; Bakak, 2016). Kernel analysis indicates the density of points falling into the circle with a defined radius and the point density that changes as they move away from this source (Silverman, 1986). The kernel density formula is expressed as follows:

$$\lambda(\mathrm{s}) = \sum_{i=1}^{n} \frac{1}{\pi r^2} k\left(\frac{d_{is}}{r}\right), \tag{10}$$

where, $\lambda(s)$, s represents the density value at position and r represents the defined radius value, n defines the total number of data set points, k represents the weight value of point i, and d_{is} defines the distance between the point and point s. In this study, earthquake density surface maps were formed considering earthquake epicenters' positions and magnitude values.

Moran's I method, having a broad scale, measures the spatial dependence level of the distribution throughout the study area. However, it cannot locally determine in which

regions the distribution is clustered within the study area. Anselin Local Moran's I is a local method used to determine clusters formed by similar and dissimilar variables. Anselin (1995) defines the Anselin Local Moran's Index as follows:

$$I_i = \frac{X_i - X}{S_i^2} \sum_{i=1, j \neq i}^{n} w_{i,j}(x_j - X), \tag{11}$$

where, x_i defines the value of the first feature in the data set and x, the mean of the relevant value (mean of earthquake magnitudes), $w_{i,j}$ represents the weight value between ith and jth data points. If the result value is statistically high, it means that high or low values also form clusters in the areas around the region. If the result value is low, it means that different values gather. The Z score value also provides information on the statistical significance of the resulting value. The P value should be small enough for the cluster or the outlier to be considered statistically significant ($p < 0.05$) (Al-Ahmadi et al., 2014; Affan et al., 2016).

The Getis-Ord Gi* method determines where the data set's hot and cold spots are clustered positionally (Getis and Ord, 1992; Ord and Getis, 1995; Mitchell, 2005; Erdogan, 2010; Al-Ahmadi et al., 2014; Affan et al., 2016; Akyurek and Arslan, 2018). The higher the statistically calculated Z score, the higher the high/warm values clustering is in the data set. On the other hand, the lower the Z score is, the greater the clustering of low values is in the data set. If the calculated Gi* value is close to zero, it can be said that there are no high or low values in the neighborhood of the calculated feature. The following formula calculates Getis-Ord Gi*:

$$G_i^* = \frac{\sum_{i=1}^{n} w_{i,j} x_j - X \sum_{j=1}^{n} w_{i,j}}{s \sqrt{\frac{\left[n \sum_{j=1}^{n} w_{i,j}^2 - \left(\sum_{j=1}^{n} w_{i,j} \right)^2 \right]}{n-1}}}, \tag{12}$$

where, x_j defines the value of the jth value in the data set, $w_{i,j}$ defines the spatial weight value/matrix between ith and jth data points (Mitchell, 2005).

4 Results and discussion

The study used data on 1234 earthquakes along the Burdur-Fethiye fault zone with a magnitude greater than 3.5 that occurred between 1914 and 2019 (Fig. 2). Statistical information on these earthquakes can be seen in Table 1.

According to Table 1, almost 70% of these earthquakes, which probably belong to seismic sequences, have a magnitude ranging between 3.5 and 4. Secondly, earthquakes with a magnitude ranging between 4.1 and 5 make up 26.25% of all these earthquakes. While 4.2% of earthquakes have a magnitude of 5.1–6, 4 earthquakes, with quite destructive effects, have occurred with a magnitude greater than 6. These 1234 earthquakes indicate that the Fethiye-Burdur fault zone is still active.

Results of the study's statistical methods, such as Quadrat Analysis, Average Nearest Neighbor, Moran's I, and Getis Ord General G, which are among the global spatial statistical methods, can be seen in Tables 2, 3, 4, and 5.

VMR value for Quadrat analysis was found to be 4.68 for all earthquake points. Since VMR is greater than 1, it indicates a clustering between earthquake epicenters. ANN, GMI, and GOGG values were found to be 0.72, 1.28, and 0.0008, respectively, and all global statistical values showed a cluster pattern for 1234 earthquakes that occurred between 1914 and 2019. A cluster indicates that earthquakes around the Fethiye-Burdur fault zone are spatially related.

Then, all global statistics methods were separately formed according to earthquake magnitude values shown in Table 1. All values in Quadrat and ANN, except for the $6.1 \leqslant M \leqslant 7.1$ magnitude value, indicated clustering (Tables 2 and 3). Clustering means an active fault with a possible short recurrence interval or domino-style triggering of a nearby segment. When earthquakes were analyzed using the GMI method, earthquakes with a magnitude of $5.1 \leqslant M \leqslant 6$ and $6.1 \leqslant M \leqslant 7.1$ showed a random distribution, whereas others showed a clustering feature (Table 4). In the GOGG method, earthquakes with a magnitude of $5.1 \leqslant M \leqslant 6$ and $6.1 \leqslant M \leqslant 7.1$ showed random distribution as was the case in the GMI method, while earthquakes with a magnitude of $3.5 \leqslant M \leqslant 4$ showed low clusters, and others; high clusters (Table 5). When global statistics methods are compared with each other, it is seen that different results are obtained. In this case, Kernel density, Anselin Local Moran's I, and Getis Ord Gi* methods were used in order

Table 1 Descriptive statistics of earthquakes that occurred in the Fethiye Burdur fault zone between 1914 and 2019

Magnitude	Earthquake Total	% of earthquakes	Minimum magnitude	Maximum magnitude	Mean magnitude	Standard deviation
$3.5 \leqslant M \leqslant 4$	854	69.2	3.5	4	3.65	0.15
$4.1 \leqslant M \leqslant 5$	324	26.25	4.1	5	4.52	0.29
$5.1 \leqslant M \leqslant 6$	52	4.2	5.1	6	5.38	0.26
$6.1 \leqslant M \leqslant 7.1$	4	0.32	6.1	7.1	6.7	0.43
$3.5 \leqslant M \leqslant 7.1$	1234	100	3.5	7.1	3.96	0.55

Table 2 Quadrat Analysis

Magnitude (M)	Quadrat Analysis			
	Average	Variance	VTMR	Pattern
3.5 ⩽ M ⩽ 4	1.19	4.30	3.59	Clustered
4.1 ⩽ M ⩽ 5	0.55	1.73	3.13	Clustered
5.1 ⩽ M ⩽ 6	0.10	0.14	1.36	Clustered
6.1 ⩽ M ⩽ 7.1	0.009	0.009	0.10	Regular
3.5 ⩽ M ⩽ 7.1	1.83	8.57	4.68	Clustered

Table 3 Average Nearest Neighbor

Magnitude (M)	Average Nearest Neighbor			
	Ratio	*z* statistic	*p*-value	Pattern
3.5 ⩽ M ⩽ 4	0.73	−14.84	0.00	Clustered
4.1 ⩽ M ⩽ 5	0.71	−10.54	0.00	Clustered
5.1 ⩽ M ⩽ 6	0.89	−1.73	0.08	Clustered
6.1 ⩽ M ⩽ 7.1	1.67	3.14	0.002	Dispersed
3.5 ⩽ M ⩽ 7.1	0.72	−18.61	0.00	Clustered

Table 4 Global Moran's *I*

Magnitude (M)	Global Moran's *I*			
	Index	*z* statistic	*p*-value	Pattern
3.5 ⩽ M ⩽ 4	0.12	1.87	0.06	Clustered
4.1 ⩽ M ⩽ 5	0.54	8.00	0.00	Clustered
5.1 ⩽ M ⩽ 6	0.11	0.29	0.77	Random
6.1 ⩽ M ⩽ 7.1	0.30	0.83	0.41	Random
3.5 ⩽ M ⩽ 7.1	1.28	29.87	0.00	Clustered

Table 5 Getis Ord General G

Magnitude (M)	Getis Ord General G			
	Index	*z* statistic	*p*-value	Pattern
3.5 ⩽ M ⩽ 4	0.0007	−2.59	0.01	Low-clusters
4.1 ⩽ M ⩽ 5	0.0031	3.60	0.0003	High-clusters
5.1 ⩽ M ⩽ 6	0.002	1.18	0.24	Random
6.1 ⩽ M ⩽ 7.1	0.000024	1.45	0.15	Random
3.5 ⩽ M ⩽ 7.1	0.0008	5.29	0.00	High-clusters

to determine the earthquake clusters in the study area on a local scale. Getis Ord Gi* statistics, by comparing the local mean with the general mean within a certain distance (or band), can determine where the high and low-value features are clustered in the study area, considering all the remaining data set features. In cases where autocorrelation is unavailable locally, or there is local variability, Anselin Local Moran's *I* is used to define attribute values with similar values in a given field. This method determines a mean value from all neighboring data set features and functions by taking the difference of neighboring values from this mean value. This principle can determine the regional neighborhoods/variations in the study area (İlci, 2013).

Figures 3 and 4 reveal the results obtained from local spatial statistics methods (Anselin Moran's *I* and Getis Ord Gi*). According to Anselin Moran's I method in Fig. 3, it can be seen that high values (HH) are clustered in the West of Burdur city center and the district of Yeşilova, whereas low values (LL) are clustered in the districts of Çameli and Altınyayla, and south of Gölhisar district. In Fig. 4, it can be seen that the Getis Ord Gi* method also provided similar results. It is seen that high values (hot spots) are clustered in the West of Burdur city center, in Yeşilova district, and south of Karaman district, whereas low values (cold spots) are clustered in Çameli and Altınyayla districts, south of Gölhisar districts, and north of Fethiye district.

The areas where earthquakes greater than 3.5 were concentrated were shown by kernel density analyses, considering the earthquake magnitudes (Fig. 5). Figure 5(a) shows the density of all earthquake data. Accordingly, the earthquake densities are mostly concentrated in the Dinar and Eğirdir districts in the northern part of the study area, Burdur city center, and Yeşilova-Acıpayam districts located in the central parts of the study

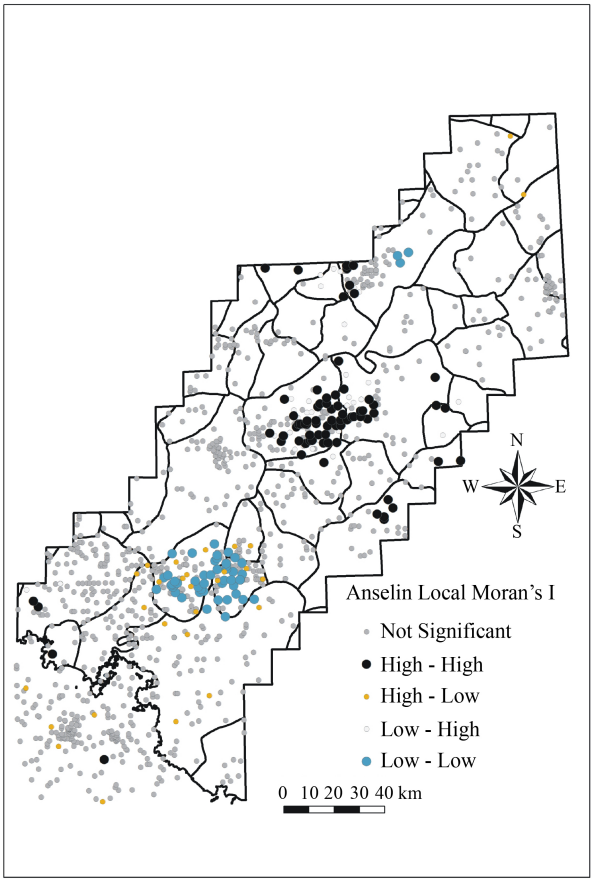

Fig. 3 Anselin Local Moran's *I* cluster analysis.

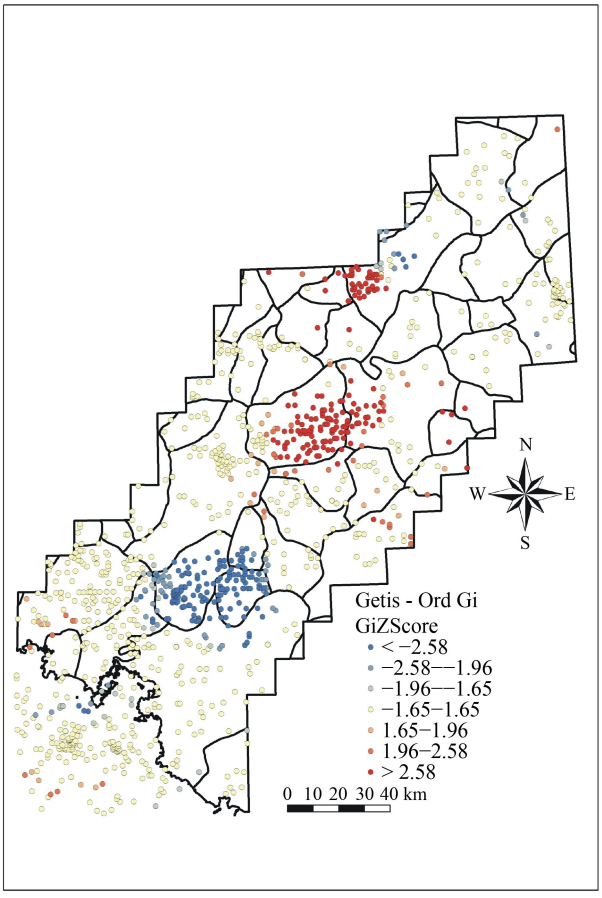

Fig. 4 Getis-Ord Gi* hot spot analysis.

area, and Çameli-Altınyayla-Köyceğiz districts located in the south-west of the study area. Figures 5(b) and 5(c) reveal that earthquakes with a magnitude of $3.5 \leqslant M \leqslant 4$ and $4.1 \leqslant M \leqslant 5.1$ have similar density areas with all earthquake data. In Fig. 5(d), it can be observed that earthquakes with a magnitude of $5.1 \leqslant M \leqslant 6$ are concentrated in the south-western part of the study area. Earthquakes greater than 6, with devastating effects, are found to be concentrated in the districts of Dinar, Burdur, Altınyayla, and offshore Gulf of Fethiye (Fig. 5(e)). The mean center, median center, standard distance, and standard deviational ellipses of earthquakes are shown in Figs. 6(a)–6(e). The magnitudes of earthquakes were used for the mean center and median center.

Accordingly, the mean center coordinates are x: 720603 and y: 4122726 for all earthquakes, whereas the median center is at the coordinates of x: 714253 and y: 4112218 (Fig. 6(a)). It is seen that the mean centers of all earthquakes with a magnitude of 3.5–6 remain within the borders of the Gölhisar district, while the mean center of earthquakes greater than 6 has occurred within the borders of the Çameli district, which is located in the south-west. On which side of the mean center are median centers located is important in providing information about the distribution direction (Tagıl and Alevkayalı, 2013). While median centers are located in the south-west of the mean center in Figs. 6(a), 6(b), and 6(e), they are located in the north-east in Figs. 6(c) and 6(d). Standard distance indicates how far the epicenters spread from the mean center.

The magnitude values of earthquakes were included in the analysis as the weight coefficient, and standard distance was obtained accordingly. A decrease in the circle signifies that the center of epicenters is within the mean value, while an increase in the circle area signifies that earthquakes are distributed throughout the region. It is seen that circles of standard distance cover the central and south-western parts of the study area. Accordingly, it can be said that earthquake epicenters are mostly clustered in these areas. When the standard deviational ellipses are analyzed, it can be seen that they are north-east-south-west trending. This is because the Fethiye-Burdur fault zone is in this direction, and earthquakes occur on this fault line (Figs. 6(a)–6(e)).

5 Conclusions

In this study, which aims to conduct a GIS-based spatial analysis of earthquakes occurring in the historical process along the Fethiye-Burdur fault zone, earthquakes with a magnitude of 3.5 and above between 1914 and 2019 were analyzed by conducting local and global spatial statistical analyses.

Quadrat analysis, ANN, GMI, and GOGG indices demonstrate that earthquakes cluster in certain regions and that these earthquakes are positionally related to each other. Anselin Moran's I local analyses show that high values (HH) are clustered in the West of Burdur city center and Yeşilova district, while low values (LL) are clustered in Çameli and Antalya districts and south of Gölhisar district. It is seen that the Getis Ord Gi* method has provided similar results and that high values (hot spots) are clustered in the West of Burdur city center, Yeşilova district, and north of Karaman district, whereas low values (cold spots) are clustered in Çameli and Altınyayla districts, south of Gölhisar district, and north of Fethiye district. According to the kernel density analysis, earthquakes greater than 5 are clustered in the central parts of the study area, in the west of Burdur province and Yeşilova district, and the south-western parts, including the districts of Çameli-Altınyayla-Gölhisar-Köyceğiz-Dalaman, and Fethiye, and offshore Gulf of Fethiye. Burdur province and Fethiye district also constitute the settlements with the highest population density (> 100000).

When the mean and median center analyses of earthquakes are analyzed, it can be seen that all the earthquake epicenters and the median centers of earthquakes with a magnitude of $3.5 \leqslant M \leqslant 4$ and $6 \leqslant M \leqslant 7.1$ are located in the south-west of the mean

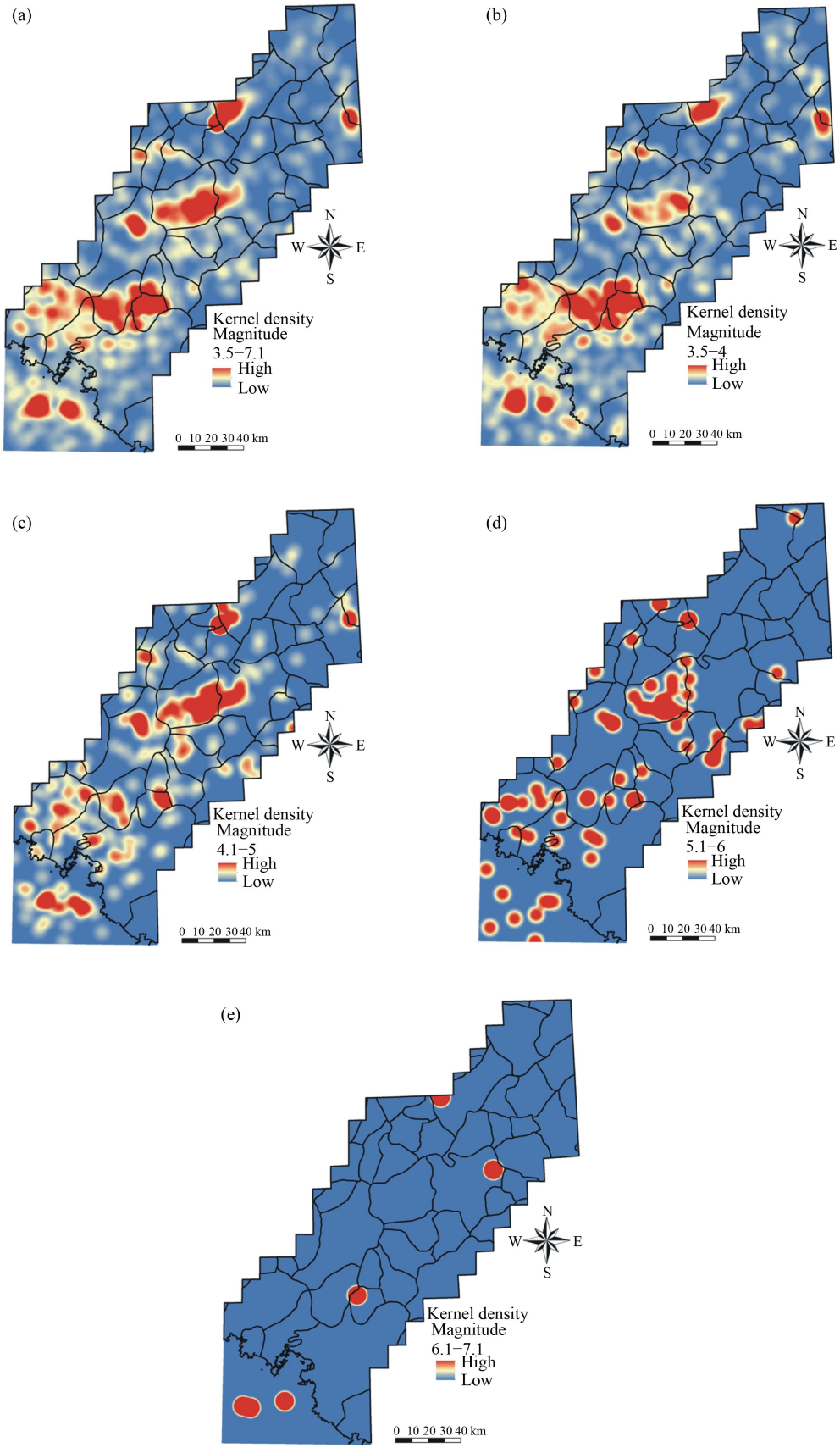

Fig. 5 Kernel density analysis (a) for all magnitudes, (b) between M = 3.5–4, (c) between M = 4.1–5, (d) between M = 5.1–6, and (e) between M = 6.1–7.1.

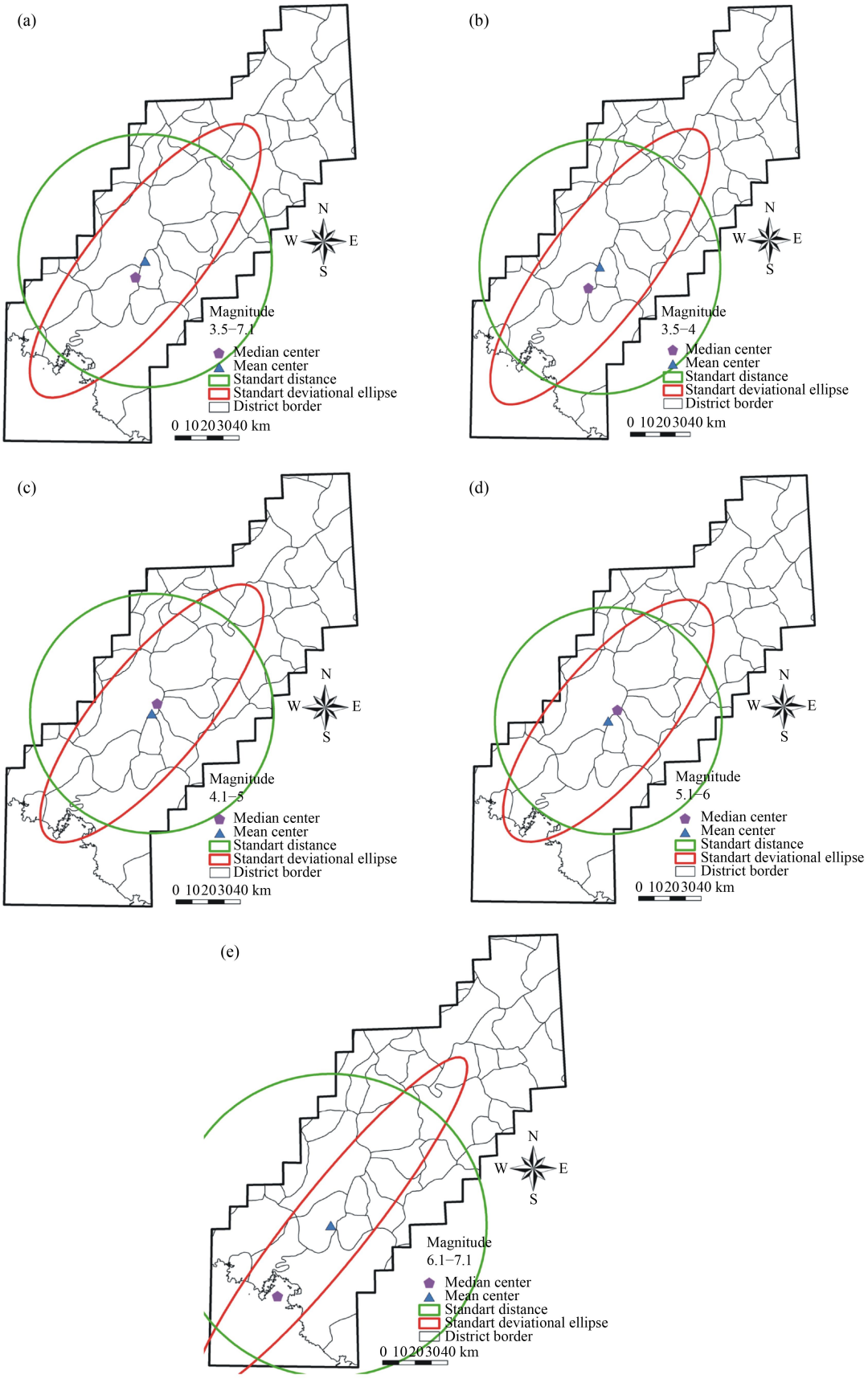

Fig. 6 Mean center, median center, standard distance, and standard deviational ellipses of earthquakes. (a) for all magnitudes, (b) between M = 3.5–4, (c) between M = 4.1–5, (d) between M = 5.1–6 and (e) between M = 6.1–7.1.

centers while the median centers of earthquakes with a magnitude of $4 \leqslant M \leqslant 6.1$ are located in the north-east of the mean centers. Accordingly, the distribution direction of epicenters is south-west-north-east trending. The fact that the standard distance circles cover the central and south-western parts of the study area has revealed that earthquakes generally spread in these areas. The fact that standard deviational ellipses are north-east-south-west trending is interpreted in a way that the Fethiye-Burdur fault line is along this direction, and earthquakes occur on this fault line.

To conduct a significant analysis of the map views and attribute data of earthquakes that occurred in the region, it is necessary to define and find relationships between them. Determining the clustering regions and density of these earthquakes positionally using the GIS, to this end, is important in terms of revealing their relationships to settlements. The fact that earthquakes have caused many losses of life and property makes the region's disaster planning and management crucial. To reduce earthquake damage in seismically active areas, it is necessary to be prepared for an earthquake and to take precautions. Owing to this study, it has been observed that spatial statistical analyses are effective methods in revealing the pattern of epicenter points in seismic activities and determining the cluster areas that mean an active fault with a possible short recurrence interval or domino-style triggering of a nearby segment.

Competing interests The authors declare that they have no competing interests.

References

AFAD (Disaster and Emergency Management Authority) (2018). Disaster management and natural disasters statistics in Turkey (in Turkish)

Affan M, Syukri M, Wahyuna L, Sofyan H (2016). Spatial statistics analysis of earthquakes in Aceh Province Year 1921–2014: cluster seismicity. Aceh Int J Sci Technol (Banda Aceh), 5(2): 54–62

Akyurek O, Arslan O (2018). Spatial statistical analysis of historical earthquakes (1900–2016) in Kocaeli Province and its surroundings. J Genomics, 3(1): 48–62 (in Turkish)

Al-Ahmadi K, Al-Amri A, See L (2014). A spatial statistical analysis of the occurrence of earthquakes along the Red Sea floor spreading: clusters of seismicity. Arab J Geosci, 7(7): 2893–2904

Ammon C J, Lay T, Simpson D W (2010). Great earthquakes and global seismic networks. Seismol Res Lett, 81(6): 965–971

Anselin L (1995). Local indicators of spatial association-LISA. Geogr Anal, 27(2): 93–115

Arslan R (2017). 1957 Fethiye earthquake and effects on region. International Periodical for the Languages, Literature, and History of Turkish or Turkic, 12(35): 33–47 (in Turkish)

Atabey E (2000). Earthquake. General Directorate of Mineral Research and Exploration Training Series, 1–71 (in Turkish)

Ayday C, Yaman N, Gocmez A (2015). Contributions to Eskisehir Province earthquake risk analysis with earthquake center data between 1900–2015. TUFUAB VIII. Technical Symposium Konya, 71–76

Bakak O (2016). The spatial evaluation of 2005 Sığacık Gulf (İzmir) earthquakes. Bulletin of the Earth Sciences Application and Research Centre of Hacettepe University, 37(1): 51–63 (in Turkish)

Barka A, Reilinger R, Şaroglu F, Şengor A M C (1997). The Isparta Angle: Its importance in the neotectonics of the Eastern Mediterranean region. International Earth Sciences Colloquium on the Aegean Region (IESCA-1995). Proc Natl Acad Sci, 1: 3–17

Bering D (1971). Lithostratigraphy, development and maritime history of the Neogene and Quaternary intramontane basins of the Pisidian lake region. Supplements to the Geological Yearbook,101. Hannover: Eren Publications (in German)

Beyhan G, Keskinsezer A (2016). Investigation of the gravity data from Fethiye–Burdur fault zone using the Euler deconvolution technique. Geomechanics Geophysics Geo-Energy Geo-Resources, 2(3): 195–201

Bozcu M, Yagmurlu F, Senturk M (2007). Some neotectonic and paleosismological features of the Fethiye-Burdur Fault zone, SW Anatolia. J Geol Eng, 31(1): 25–48 (in Turkish)

Bufe C G, Perkins D M (2005). Evidence for a global seismic-moment release sequence. Bull Seismol Soc Am, 95(3): 833–843

Danese M, Lazzari M, Murgante B (2008). Kernel density estimation methods for a geostatistical approach in seismic risk analysis: The case study of Potenza Hilltop Town (Southern Italy). International Conference on Computational Science and Its Applications Perugia, Italy: Lecture Notes in Computer Science, 415–429

Erdogan S (2010). GIS applications in epidemiology: A comparison of spatial clustering methods-example of Meningococcal. Electron J Math Technol, 2(2): 23–31 (in Turkish)

Getis A, Ord J (1992). The analysis of spatial association by use of distance statistics. Geogr Anal, 24(3): 189–206

Hall J, Aksu A E, Elitez I, Yaltırak C, Cifci G (2014). The Fethiye-Burdur fault zone: A component of upper plate extension of the subduction transform edge propagator fault linking Hellenic and Cyprus Arcs, Eastern Mediterranean. Tectonophysics, 685: 80–99

İlci V (2013). Determination of traffic hotspots using spatial statistical methods: Case study Afyonkarahisar-Konya. Afyon Kocatepe University Graduate School of Natural and Applied Science, 1–108

Kagan Y Y, Jackson D D (1991). Seismic gap hypothesis ten years after. J Geophys Res, 96(B13): 21419–21431

Karaman M E (1986). Seismicity of settlement areas in and around Burdur Province. Bulletin of Turkish National Committee of Engineering Geology, 23–30 (in Turkish)

Karaman M E (1990). Basic geological characteristics of southern Isparta. Geological Bulletin of Turkey, 33: 57–67 (in Turkish)

Kasap R, Gurlen U (2003). Obtaining the return period of earthquake magnitudes: As an example Marmara Region. Doguş University Journal, 4(2): 157–166 (in Turkish)

Koçyigit A (1983). Tectonics of the Hoyran Lake (Isparta Bend) region. Bulletin of the Geological Society of Turkey, 26: 1–10 (in Turkish)

Koukouvelas I, Aydın A (2002). Fault structure and related basins of

the North Aegean Sea and its surroundings. Tectonics, 21(5): 1–17

Lee J, Wong D W (2001). Statistical Analysis with Arcview GIS. Canada: John Wiley & Sons Inc

McClusky S, Balassanian S, Barka A, Demir C, Ergintav S, Georgiev I, Gurkan O, Hamburger M, Hurst K, Kahle H, Kastens K, Kekelidze G, King R, Kotzev V, Lenk O, Mahmoud S, Mishin A, Nadariya M, Ouzounis A, Paradissis D, Peter Y, Prilepin M, Reilinger R, Sanli I, Seeger H, Tealeb A, Toksöz M N, Veis G (2000). Global positioning system constraints on plate kinematics and dynamics in the eastern Mediterranean and Caucasus. J Geophys Res, 105(B3): 5695–5719

McKenzie D (1978). Active tectonics of the Alpine-Himalayan belt: The Aegean Sea and surrounding regions. Geophys J Int, 55(1): 217–254

Mitchell A (2005). The ESRI Guide to GIS Analysis, Spatial Measurements, and Statistics. Redlands California: ESRI Press

Ord J, Getis A (1995). Local spatial autocorrelation statistics: distributional issues and an application. Geogr Anal, 27(4): 286–306

Ozata M (2009). Burdur History from Antiquity to the War of Independence. İzmir: Umay Press,1–262 (in Turkish)

Ozyıldıran G (2015). Reconstruction after 1971 Burdur earthquake. International Burdur Earthquake & Environment Symposium (IBEES). Mehmet Akif Ersoy University Burdur, 311–321 (in Turkish)

Price S, Scott B (1994). Fault-block rotations at the edge of a zone of continental extension; southwest Turkey. J Struct Geol, 16(3): 381–392

Senturk M (2003). Seismotectonic features of the region between Acıgöl and Burdur Lakes. Isparta Master Thesis Süleyman Demirel University Institute of Science, 1–83 (in Turkish)

Sezer C (2014). Ottoman Red Crescent Association's Aid in 1914 Isparta-Burdur Earthquake. J Suleyman Demirel University Institute Social Sci, 1(19): 17–34 (in Turkish)

Silverman B (1986). Density estimation for statistics and data analysis. London: Chapman & Hall, 1–175

Stein R S, Barka A A, Dieterich J H (1997). Progressive failure on the North Anatolian fault since 1939 by earthquake stress triggering. Geophys J Int, 128(3): 594–604

Tagıl S, Alevkayalı Ç (2013). Earthquake spatial distribution in the Egean Region, Turkey: The Geostatistical approach. J Intern Social Res, 6(28): 369–379 (in Turkish)

Tan O, Tapırdamaz M C, Yoruk A (2008). The earthquake catalogues for Turkey. Turk J Earth Sci, 17(2): 405–418 (in Turkish)

Taymaz T, Price S (1992). The 1971 May 12 Burdur earthquake sequence, SW Turkey: A synthesis of seismological and geological observations. Geophys J Int, 108(2): 589–603

Tiryakioglu İ, Floyd M, Erdogan S, Gulal E, Ergintav S, McClusky S, Reilinger R (2013). GPS constraints on active deformation in the Isparta Angle region of SW Turkey. Geophys J Int, 195(3): 1455–1463

UCLEA (2012). Turkey's Earthquake Fact and the Chamber of Mechanical Engineers Chamber's Recommendations. Chamber of Mechanical Engineers, Ankara. Press No: MMO, 587: 1–78 (in Turkish)

Woo G (1996). Kernel estimation methods for seismic hazard area source modeling. Bull Seismol Soc Am, 86(2): 353–362

Yagmurlu F (2000). Seismotectonic features of the Burdur fault. Seismicity of Western Anatolia Symposium İzmir: Izmir governorship, 143–152 (in Turkish)

Yılmaz Y (2000). Active tectonics of the Aegean Region. In: Seismicity Symposium of Western Anatolia, Proceedings Book, 3–14